ERROR ANALYSIS OF AIRBORNE MULTISENSORY SYSTEMS

C. Toth and D. Grejner-Brzezinska

The Center for Mapping
The Ohio State University
470 Hitchcock Hall, 2070 Neil Avenue, Columbus, OH 43210
toth@cfm.ohio-state.edu

KEY WORDS: Error propagation, Sensor and system calibration, Digital camera, LiDAR, Georeferencing

ABSTRACT:

One aspect of the recent paradigm shift in geospatial information sciences is that data acquisition and processing systems have moved away from the single sensor-based model to advanced integrated multisensory systems, which typically include imaging and navigation sensors. Active sensors, such as Light Detection and Ranging (LiDAR) and Interferometric Synthetic Aperture Radar (IFSAR), are routinely used with conventional optical sensing where a new generation of high-performance digital camera systems have been developed in the past few years. The direct georeferencing of the remote sensing platform is usually provided by state-of-the-art navigation technology based on the Global Positioning System/Inertial Measurement Unit (GPS/IMU).

As the number of sensors has increased, the error budget calculations for derived geospatial products has become more complex; the number of contributing terms has shown a multi-fold increase. The focus of calibration has shifted from individual sensor calibration to system calibration to consider interrelationships between multiple sensors. At the system calibration level, even the error contributions of in-scene objects play an increased role and must be more carefully considered. Research to date has been primarily focused on individual sensor calibration or calibration of a pair of sensors. The objective of this investigation is to combine the effects of all the sensor and sensor-related errors to obtain the overall error budget of airborne remote sensing sensor suites. The error budget should include all navigation errors, imaging sensor modeling errors, inter-sensor calibration errors, and object space characteristics.

1. INTRODUCTION

Airborne surveying and remote sensing technology has seen significant developments in the past decade, resulting in a paradigm shift in mapping (Grejner-Brzezinska *et al.,* 2004). State-of-the-art airborne multisensory imaging systems are extremely powerful tools used to acquire highly accurate geospatial data in large volumes. The complexity of these systems, however, also presents several challenges, including the proper calibration of the sophisticated sensor systems and, consequently, reliable validation or characterization of the data accuracy. The wide-spread use of direct georeferencing of the sensor platform makes the system calibration even more crucial, as, in general, no provision can be made for incorrect sensor models; note that indirect sensor orientation, such as AT, can absorb sensor modeling errors.

Modern airborne mapping systems typically include a combination of navigation and imaging sensors. The most popular combinations are the GPS/IMU-supported large-format digital camera or LiDAR systems. In most installations, the LiDAR systems include a fourth sensor, a medium-format digital camera, though in many high-end configurations large-format digital cameras are already increasingly used. With three or four integrated sensors, the error budget calculations for any derived geospatial product, such as 3D point positioning accuracy from stereo imagery or LiDAR point cloud characterization, has become more complex, as the number of contributing terms has shown a multi-fold increase. While research has been addressing multisensory system calibration for many years, typically not all the sensors are simultaneously considered. Furthermore, limited or no attention is paid to impact of the object space. This study elaborates on a model which attempts to incorporate the effects of all the sensor and sensor-related errors, as well as object space characteristics, to obtain the overall error budget of airborne multisensory remote sensing systems.

2. STATE-OF-THE-ART IN MULTISENSOR ERROR ANALYSIS

Most of the work on multisensory system calibration and performance evaluation is based on the typical configuration of GPS/IMU aiding a digital camera system (Ip *et al.*, 2007; Blazquez, 2008) and addresses the direct georeferencing (DG), also called direct sensor orientation (DSO), case (Toth and Brzezinska, 1998). Integrated sensor orientation (ISO) is a combination of DG and indirect sensor orientation; note that the latter one had been the practice in airborne surveying until GPS was introduced (Ackermann and Schade, 1993). The differences between indirect sensor orientation and direct sensor orientation techniques are typically compared to the behavior of interpolation and extrapolation, respectively (Habib and Schenk, 2001; Cramer and Stallmann, 2002; Yastikli and Jacobsen, 2005). Since ISO is practically limited to frame camera sensor models, thus excluding LiDAR, IfSAR, and practically most pushbroom camera model-based systems, and ISO has better error characteristics. The error analysis of the DG method-based multisensory systems is of main interest in practice.

Publications on the performance evaluation of multisensory systems generally fall into three categories: (1) manufacturer's specification, such as error terms for georeferencing and LiDAR systems, or factory camera calibration results, (2) independent calibration results and performance assessment by major organizations, such as the USGS (U.S. Geological Survey) in North America and EuroSDR (European Spatial Data Research) in Europe, and (3) performance reports and analysis based results obtained in various mapping projects, usually provided by geospatial data provider companies. All these publications and reports provide valuable information about the theoretical achievable and empirically realizable point positioning accuracy. However, a direct comparison between any two categories typically shows a discrepancy, which may not mean that one or more of the results are incorrect, rather it only indicates that different methodologies were used and/or the experiments were performed under different circumstances and environments. In the following, a short review is provided on the three sensor systems, and then the inter-sensor relationship is discussed.

2.1 Direct georeferencing systems

The performance of DG systems is rarely validated independently, as it would require the use of totally independent systems that have about an order better performance, which is neither practical nor affordable. Therefore, the performance terms are derived from the specification of the sensor manufacturer, such as IMU drift and noise parameters, and/or internally estimated from navigation filter solutions (Extended Kalman Filter). Since high-resolution digital camera imagery can provide for excellent accuracy at large scale, they are frequently used for georeferencing performance evaluation. Manufacturers' quoted specifications for their highest performance airborne georeferencing systems are listed in Table 1; note all of them are based on post-processed solutions.

The listed parameters from the four vendors are quite comparable, which is due to two things. First, the very same GPS positioning method is used in all cases, and, in GPS/IMU integration, the GPS performance defines the absolute accuracy; more on GPS accuracy can be found in (Raquet, 1998). Second, very similar, tactical grade, IMU's are employed in all systems, so assuming comparable GPS solution, the attitude terms should be also close to each other.

2.2 Digital camera systems

Most of the high-performance airborne digital large-format camera systems are based on the frame model, though pushbroom or three-line camera model-based systems are also widely used; for summary of the digital camera market, see (Gordon and Walker, 2007). In all cases, these systems can be considered multisensory, as they are typically built from several sensors, such as multiple camera heads with their own lenses or multiple imaging sensors sharing one optical system. Because of their design, the former collimator based calibration methods, widely used for analog cameras, are not always applicable to digital cameras, and consequently, manufacturers had to implement their own calibration process, which includes both the geometrical and radiometric characterization of the system. In many respects, these processes go far beyond just camera calibration, as in most cases, a synthetic image is formed from the individual camera/sensor heads. Lens distortion is usually removed and several parameters of the resulting pin-hole camera model can be arbitrarily set. Table 2 shows the virtual parameters of the camera model of the Microsoft UltraCamX (Microsoft, 2008) and the Intergraph DMC systems (Intergraph, 2009); similar calibration results are available for the Leica ADS80 line camera (Leica, 2009). The accuracy of the parameters is typically reported in the 1-2μ range. A recent comprehensive evaluation of state-of-the-art airborne digital camera systems can be found in (Jacobsen *et al.*, 2010).

Parameter	**UltraCamX**	**DMC**
Focal length [mm]	100.5	120
Sensor size [pixel]	14,430 x 9,420	13,824 x 7,680
Pixel size [μ]	7.2	12
Principal point [mm]	0	0
Lens distortion	n/a	n/a

Table 2. Typical frame camera model parameters (virtual).

In addition to the error contribution of the camera model, the actual geospatial data extraction performance of digital camera systems depends heavily on the image measurement accuracy, which itself depends on the radiometric performance of the camera and the image content. Obviously, the first component can be calibrated, and, in fact, most state-of-the-art cameras come with their radiometric calibration protocol. The image measurement dependency on object space, however, cannot be generally characterized, as the image quality can vary over a larger range, based on light conditions, object surface, and texture. In addition, there is a difference in image measurement accuracy between operator-measured and automatically measured points. While manual measurements are relatively consistent for both control and tie points, the matching performance for tie points depends a lot on image texture. Figure 1 shows manual measurement performance for all the high-end frame digital cameras; the results are from a German camera evaluation project (Haala et. al., 2010). Since the experiment was performed in a controlled environment in cooperation with several research institutes, the results could be considered as a lower bound for achievable image measurement accuracy. Note, automatically matched points typically exhibit a bit higher performance for images with simple complexity and good texture, but the performance falls below the manually matched for images with difficult object content and less favourable texture.

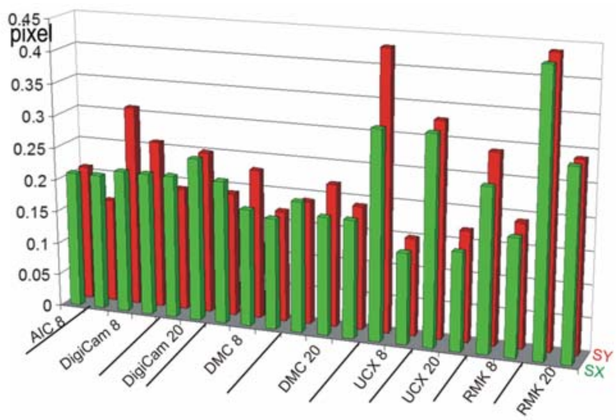

Figure 1. Standard deviation of manual image point measurements (Haala *et. al.*, 2010).

	Applanix AV 610	AEROControl-III	Leica IPAS20 CUS6	Novatel SPAN
Position (m)	0.05-0.30	0.05	0.05-0.30	0.01-0.02
Velocity (m/s)	0.0050	0.005	0.0050	0.010
Roll and pitch (°)	0.0025	0.003	0.0025	0.005
True heading (°)	0.0050	0.007	0.0050	0.008

Table 1. Specification of high-end airborne georeferencing systems parameters.

The ultimate point positioning accuracy of using images of a digital camera system depends on the image geometry too. In most cases, stereo-imagery and, in growing number recently, multiple image coverage (multi-ray imagery) are used to extract 3D object coordinates. The geometry in both cases, such as image overlap for a stereo image pair or point location within the image, impacts the achievable accuracy, which is well known from photogrammetry (Kraus, 1992). In addition, if multiple images are used, the dynamic content of the object space can further cause problems, as the established geometry between sensors or images taken at different times strictly applies only to the static component of the object space. Matching any kinematic objects in the scene, such as moving vehicles, people, animals or even vegetation in wind, will not satisfy the established geometrical model.

2.3 LiDAR systems

The calibration and performance characterization of LiDAR systems are much more complicated or rather challenging than that of digital cameras or georeferencing systems. The reason is that there are several sources of errors from the system, including LiDAR platform georeferencing accuracy, the laser ranging accuracy, and the effect of the mechanical scanning; and, in addition, the derived LiDAR product, the point cloud, significantly depends on object space circumstances and the environment. Consequently, the calibration process is not straightforward, and both physical model-based and data-driven approaches are used. In the last comprehensive review of the major LiDAR products, published in (GIM, 2009), the "Precision and Resolution" group shows the largest variety among all the parameters, clearly indicating that the performance characterization is not simple, as it depends on so many factors. This fact, in turn, emphasizes why LiDAR users need good QA/QC procedures, as the point cloud just cannot be characterized based only on manufacturers' specification.

In theory, the LiDAR equation can be used to create calibration methodologies and then to perform *in situ* calibration of LiDAR systems (Morin, 2002; Skaloud and Lichti, 2006; Habib *et al.,* 2007). Since most calibration processes would require access to sensor level (raw) data, which is not always available (as most systems work as black-box for the user), strip adjustment has gained popularity among LiDAR users as a tool to support QA/QC. Practically, discrepancies observed between overlapping strips are identified and then a geometrical model is estimated, which is then applied to the point cloud to eliminate the difference. Early methods focused only on the vertical components (Killian *et al.,* 1996; Crombaghs *et al*., 2000; Kager and Kraus, 2001). Once the quality of LiDAR data improved, in terms of point density and ranging accuracy, 3D strip adjustment techniques were introduced (Maas, 2002). The next step in the evolution of strip adjustment was the introduction of the sensor model (the LiDAR equation); in other words, instead of using a data fitting approach, the observed differences were used to adjust some of the sensor parameters to remove the strip discrepancies (Behan *et al*., 2000; Burman, 2002). While earlier methods provided very little modeling of the LiDAR point cloud, the current trend is to extract features and use those for matching and, subsequently, observe discrepancies. Using the coplanarity observation equation, least squares adjustment can be formed for the sensor model using surface patches (Pothou *et al*., 2008); man-made objects, such as roofs (Glennie, 2007), or planar patches in photogrammetric and LiDAR data (Habib *et al.*, 2007). In addition, direct techniques, such as surface patches matched by ICP, can be used to establish correspondence between LiDAR strips.

To illustrate the strong dependency of the point cloud on object space condition, three error sources of importance are briefly mentioned here. Figure 2 shows the consequence of the surface orientation, or more precisely, the effect of the footprint size of the laser beam, which depending on the distance between the sensor and surface, and combined with the incident angle, can be significant.

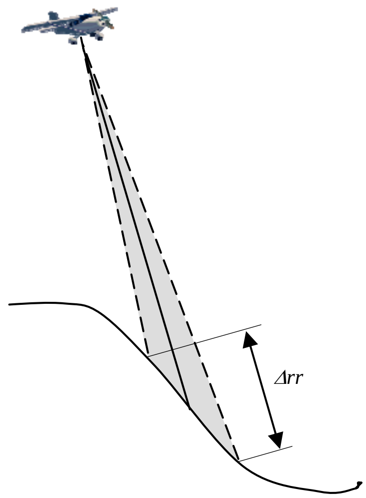

Figure 2. The impact of footprint (beam divergence) and incident angle on range measurement accuracy.

The microstructure of the surface, such as surface type, diffuse or specular, reflectivity, and land cover, impacts the laser ranging error. While, in general, it only adds to the noise level of the range data for surfaces with extreme reflectivity, the bias component could be significant too. In fact, there are intensity-based range corrections, mostly applied in transportation applications, where retro-reflective materials are widely used. Figure 3 shows typical RMSE values, obtained from several LiDAR mapping projects; the range for the five classes varies from 3 to 30 cm.

In urban areas, where there are many complex man-made objects, which are formed by planar surfaces in a structured way, multipath can be frequent; note that the specular reflection from a glass-covered building surface is prevalent in high-rise environment. Figure 4 illustrates the potential for multiple laser returns and the possibility to obtain an incorrect range measurement.

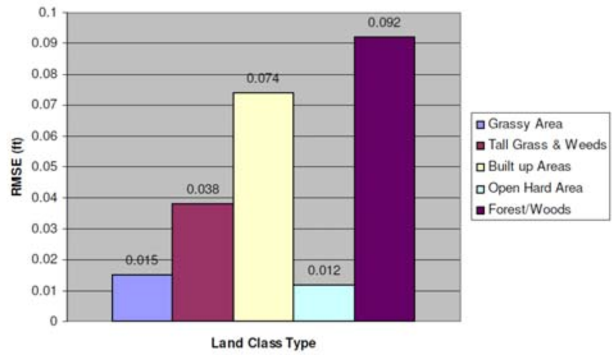

Figure 3. RMSE by land class type (AeroTec, 2007).

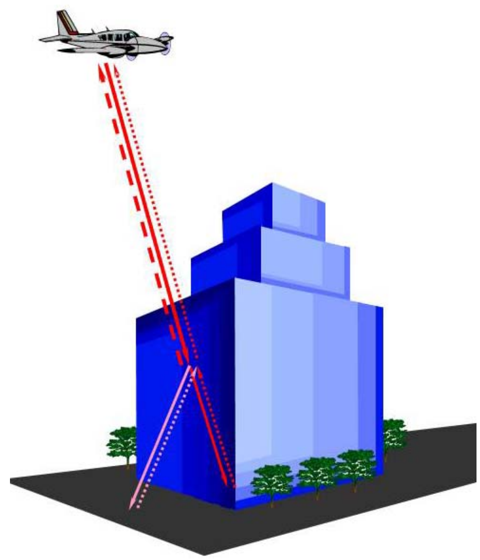

Figure 4. Laser beam multipath in urban area.

2.4 Integrated sensor performance evaluation

Research and applications on multisensory system calibration have started to increase recently. Typically, either a digital camera or a LiDAR system is combined with a GPS/IMU-based georeferencing system, and the calibration is primarily focused on the inter-sensor calibration, while the individual sensor calibration parameters are typically only refined, at best. In many cases, the objective is to obtain or improve the boresight calibration, the orientation of the imaging sensor in the navigation frame. This is essential for both imaging sensors, as any angular misalignment directly translates to errors on the ground, which effect is amplified by flying height. Note that any inaccuracy of the sensor position in the navigation frame, also called mounting bias or offset, has the same effect on the ground regardless of the flying height, and these parameters can be relatively easily and accurately measured. There are many difficulties of performing multisensory calibration and only one is mentioned here, the observability of the physical model parameters, also called the functional correlation of the model parameters. There are several approaches to mitigate this problem, but, in general, proper planning of the flight path and image overlap can usually provide for robust and reliable solution.

Representative discussions on system calibration of GPS/IMU-based direct georeferencing with digital camera and LiDAR systems can be found in (Ip *et al.*, 2007) and (Goulden and Hopkinson, 2010), respectively. In both cases, little or no attention is paid to the object space conditions and environment, which is understandable from the point of view that the objective is to obtain the best calibration parameter estimates. However, this somewhat limits the use of the results, as there is no simple way to generalize to a variety of real life conditions, where most of the mapping surveys take place.

3. CONCEPT OF ERROR ANALYSIS OF AIRBORNE MULTISENSORY SYSTEMS

Research on developing an error budget to characterize point positioning performance, based on the individual error characterization of all error sources of multisensory systems, has been limited so far. The likely reason could be the complexity of the analytical model, which is highly non-linear and has a large number of error terms. In addition, obtaining realistic error terms of the various sensors is also a challenge. The first results on comprehensive error analysis, based on rigorous error propagation, were reported in 2007, when May provided both analytical and simulated solutions for both digital frame camera and LiDAR systems, and Glennie developed the same model for LiDAR and tested it against real data. The difference in their models is that Glennie uses 14 error terms, while May excludes the mounting offset of the laser sensor and uses 11 parameters; note that the excluded parameters can be accurately measured in conventional way. A very recent publication (Goulden and Hopkinson, 2010) deals also with the LiDAR sensor, but uses a reduced set of error terms. Except for mentioning the impact of the footprint, the laser beam divergence, it is not directly included in the above models. Similarly, the impact of the object space conditions is not considered. We propose a further generalization of the rigorous error propagation model in two aspects: (1) combine the treatment of digital camera and LiDAR sensors, and (2) include corrections for object space conditions.

The direct georeferencing equation for point positioning can be formulated as:

$$r_M(t_p) = r_{M,INS}(t_p) + R_{INS}^{M}(t_p)\cdot(R_I^{INS}\cdot r_i(t_p) + b_{INS}) \qquad (1)$$

$r_M\,(t_p)$	—	3D coordinates of the point in the mapping frame
$r_{M,INS}\,(t_p)$	—	3D INS coordinates (origin) in the mapping frame, provided by GPS/INS (the navigation solution typically refers to the origin of the INS body frame)
$R_{INS}^{M}\,(t_p)$	—	Rotation matrix between the INS body and mapping frame
R_I^{INS}	—	Boresight matrix between the image sensor frame and INS body frame
$r_i\,(t_p)$	—	Range measurement (distance from laser sensor reference point to object point)
b_{INS}	—	Boresight offset vector (vector between iamge sensor reference point and the origin of INS) defined in the INS body frame

Where the imaging sensor coordinates could be obtained as shown in (2) and (3), for LiDAR and digital camera, respectively:

$$r_i(t_p) = \begin{bmatrix} 0 \\ \sin(\beta(t_p)) \\ \cos(\beta(t_p)) \end{bmatrix} \cdot d_L(t_p) \qquad (2)$$

$$r_i(t_p) = s \cdot \begin{bmatrix} x_i \\ y_i \\ -f \end{bmatrix} \qquad (3)$$

$d_L\,(t_p)$	—	Range measurement (distance from laser sensor reference point to object point)
$\beta(t_p)$	—	Scan angle defined in the laser sensor frame (x_L is flight direction, y_L to the right, and z_L goes down)
x_i, y_i	—	Image coordinates
f, s	—	Scale, focal length

Note that time is included in the above model, though it can be ignored in most applications. In addition, quantization error terms are excluded.

To compute the error budget of the mapped point, the non-linear equation (1) must be linearized by truncating a Taylor series expansion after the first term. Applying the law of error propagation to the covariance matrix of the error sources listed, the covariance matrix of the 3D point position is described by the following equation:

$$C_i = ACA^T \qquad (4)$$

where, C_i is the covariance matrix of the point coordinates (3 x 3), C is the covariance matrix of all the contributing error terms (n x n), and A is the Jacobian matrix containing the partial derivatives of the X,Y, Z point coordinates with respect to the different random variables in the georeferencing equation (3 x n). Since the error terms are usually independent, C is simplified to the diagonal elements. Depending on the number of error terms considered in (1), the analytical derivation may be quite complex, though using symbolic processing it can be easily obtained by several software packages, such as Matlab. Another possibility to deal with the problem is if a Monte Carlo simulation is performed, so C_i is empirically estimated.

The inclusion of object space conditions into the above error propagation-based model is not straightforward in the general case. The problem can be divided into two parts: (1) identification of object space conditions to be considered, and (2) modeling of the selected phenomenon to integrate it into the error budget discussed above. To illustrate the concept, the impact of the surface orientation, α_n, and scan angle, β_s, on LiDAR point positioning accuracy is considered; this is a simplified approach but can be easily generalized. The rigorous error budget provides the error terms for C_i in the nominal case of assuming horizontal object surface; note that the impact of the scan angle is already in the error budget. Based on the LiDAR sensor attitude and scan angle, a rotation matrix, R_i, can be computed that rotates from the mapping frame to a frame in which the Z axis is in the laser beam direction. Applying this rotation to C_i will result in:

$$C_i^{'} = R_i C_i R_i^T \tag{5}$$

Since the footprint is affected by the incidence angle, δ_i which can be computed from the known surface normal, attitude and scan angles, the Z variance term of C_i'can be modified as:

$$\sigma_z^{'} = \frac{\sigma_z^{'}}{\cos(\delta_i)} \tag{6}$$

Then applying the inverse of the rotation, the updated covariance matrix of the point can be computed as:

$$C_i = R_i^T C_i^{'} R_i \tag{7}$$

For a general case, if the impact of the object space condition can be modeled with a covariance matrix, then it can be directly combined with original covariance matrix of the point. If bias exists, then it can be considered in the model. Note that bias was not considered in (1), as the assumption was that all systematic errors have been removed during the individual sensor calibration.

4. SUMMARY

The concept of introducing object space conditions into the error propagation-derived error budget of airborne multisensory imaging systems offers the potential for better geospatial product characterization. More importantly, it allows for individual point error characterization and factors in the object space conditions. The model is based on the direct georeferencing equation and able to handle different imaging sensors. In the analytical derivations only random errors were considered, if the system is known to have a bias with known magnitude, its effect can also be considered; this bias (squared) can then be added to the derived variance from the random error propagation, and the MSE of point positioning can be determined. Research on the inclusion of the object space parameters is an ongoing effort, and results will be reported in the future publications.

REFERENCES

Ackermann, F. and Schade, H. 1993. Application of GPS for aerial triangulation. *Photogrammetric Engineering and Remote Sensing,* Vol. 59(11), pp. 1625–1632.

AeroTec, 2007. LiDAR Vertical Accuracy Assessment Report.

Applanix, 2007. Applanix POSAV Specification.

Blazquez, M. 2008. A New Approach to Spatio-Temporal Calibration of Multi-Sensor Systems, *International Archives of the Photogrammetry*. Vol. XXXVII. Part B1., pp. 481-486.

Burman, H., 2002. Laser strip adjustment for data calibration and verification. *International Archives of Photogrammetry and Remote Sensing*, 34 (Part 3A): 67-72.

Cramer, M. 2009. EuroSDR Network: Digital Camera Calibration Final Report, European Spatial Data Research.

Cramer, M. (2009). "The EuroSDR Performance Test for Digital Aerial Camera Systems."

Cramer M., and Stallmann D., 2002. System calibration for direct georeferencing. *International Archives on Photogrammetry and Remote Sensing*, Volume XXXIV, Com. III, Part A, pages 79-84, ISPRS Commission III Symposium, Graz, September 2002.

Crombaghs, M.J.E., Brügelmann, R., and de Min, E.J., 2000. On the adjustment of overlapping strips of laseraltimeter height data. *International Archives of Photogrammetry and Remote Sensing*, 33, (Part B3/1):224-231.

Csanyi May, N. 2008. A Rigorous Approach to Comprehensive Performance Analysis of State-of-the-Art Airborne Mobile Mapping Systems, PhD dissertation, The Ohio State University.

GIM International Product Comparison. 2009. http://www.gim-international.com/productsurvey/id31-Airborne_Lidar_Sensors,_February.html

Glennie, C. 2007. Rigorous 3D Error Analysis of Kinematic Scanning LiDAR System, *Journal of Applied Geodesy*, JAG, 1:3, pp. 147–157.

Goulden, T. 2009. Prediction of Error due to Terrain Slope in LiDAR Observations, Geodesy and Geomatics Engineering UNB.

Goulden, T. and C. Hopkinson 2010. "The Forward Propagation of Integrated System Component Errors within Airborne Lidar Data." *Photogrammetric Engineering and Remote Sensing* 76(5): 589-601.

Grejner-Brzezinska, D. A., R. Li, N. Haala and C. Toth, 2004. From Mobile Mapping to Telegeoinformatics: Paradigm Shift in Geospatial Data Acqusition, Processing, and management. *Photogrammetric Engineering & Remote Sensing*, Vol. 70, No 2, February 2004, pp. 197-210.

Haala, N., *et al.*, 2010. The German Camera Evaluation Project - Results from the Geometry Group. ISPRS Commission I Meeting, Calgary, Canada.

Habib A., Schenk T., 2001: Accuracy Analysis of Reconstructed Points in Object Space from Direct and Indirect Exterior Orienation Methods, OEEPE Workshop on Integrated Sensor Orientation. Hannover, Germany, 17-18 September, 2001.

Habib, A. 2009. Accuracy, Quality Assurance, and Quality Control of LiDAR Data. Topographic Laser Ranging and Scanning/Principles and Processing, Eds. J. Shan and C. Toth.

Habib, A., *et al*., 2007. LiDAR System Self-Calibration Using Planar Patches from Photogrammetric Data. The 5th International Symposium on Mobile Mapping Technology.

Habib, A., *et al.*, 2010. Alternative Methodoloiges for the Internal QC of Parallel LiDAR Strips, *IEEE Transactions and Remote Sensing,* Vol. 48.

Hopkinson, C., *et al*., 2005. Vegetation class dependent errors in lidar ground elevation and canopy height estimates in a boreal wetland environment. *Canadian Journal of Remote Sensing*, 31(2): 191-206.

IGI. 2010. IGI AEROcontrol Specification.

Ip, A.W.L.,N. El-Sheimy, and M.M.R. Mostafa, 2007. Performance analysis of integrated IMU/DGPS systems for mobile mapping systems. Advances in Mobile Mapping Technology-Tao & Li, 2007 Taylor & Francis Group, London.

Jacobsen, K., *et al*., 2010. DGPF-Project: Evaluation of Digital Photogrammetric Camera Systems - Geometric Performance. *Photogrammetrie Fernerkundung Geoinformation* (2): 83-97.

Jutzl, B. Gross, H. 2010. Investigations on Surface Reflection Models for Intensity Normalization in Airborne Laser Scanning (ALS) Data. *Journal of Photogrammetry and Remote Sensing*.

Kager, H., Kraus, K., 2001. Height discrepancies between overlapping laser scanner strips. *Proceedings of Optical 3D Measurement Techniques V*, Vienna, Austria: pp. 103-110.

Kilian J., Haala, N., and Englich, M., 1996. Capture and evaluation of airborne laser scanner data. *International Archives of Photogrammetry and Remote Sensing*, 31 B3, pp. 383-388.

Kraus, K., 1992, Photogrammetry, Dummler Verlag.

Leica. 2009. ADS80 Calibration Certificate.

Maas, H.-G., 2002. Methods for Measuring Height and Planimetry Discrepencies in Airborne Laserscanner Data. *Photogrammetric Engineering & Remote Sensing*, Vol. 68, No. 9. pp. 933-940.

Microsoft-Photogrammetry, 2008. UCX Camera Calibration Report.

Nayegandhi, A. 2007. USGS - LiDAR Technology Overview.

Gordon, P., Walker, A.S., 2007. Airborne Digital Imaging Technology: A New Overview, *Photogrammetric Record*, Vol. 22, No. 119, p. 203-225. 2007.

Pothou, A., *et al*., 2008. An Approach to Optimize Reference Ground Control Requirements for Estimating LiDAR/IMU Boresight Misalignment. *International Archives of Photogrammetry and Remote Sensing,* Beijing 2008.

Raquet, J. F., Development of a Method for Kinematic GPS-Carrier Phase Ambiguity Resolution Using Multiple Reference Receivers, Ph.D. Thesis, The University of Calgary.

Toth, C.K. 2009. The State-of-the Art in Airborne Data Collection Systems – Focused on LiDAR and Optical Imagery, Wichmann Verlag, pp. 147-161.

Toth, C. 2009. Strip Adjustment and Registration. Topographic Laser Ranging and Scanning/Principles and Processing, Eds. J. Shan and C. Toth.

Toth, C., Grejner-Brzezinska, D. A., 1998. Performance Analysis of the Airborne Integrated Mapping System (AIMS™), *International Archives of Photogrammetry and Remote Sensing*, Vol. XXXII, part 2, pp.320-326.

Intergraph. 2009. DMC Calibration Certificate, Carl Zeiss Jena.

Yastikli, N. and K. Jacobsen, 2005. Influence of System Calibration on Direct Sensor Orientation. *Photogrammetric Engineering & Remote Sensing*, Vol. 71, No. 5, May 2005, pp. 629-633.